IOSR Journal Of Humanities And Social Science (IOSR-JHSS)
Volume 29, Issue 1, Series 5 (January, 2024) 25-35
e-ISSN: 2279-0837, p-ISSN: 2279-0845.
www.iosrjournals.org

Mapping Tomorrow's City: Cellular Automata Based Sleuth Model Predictions For Urban Growth In Mysuru, India

Manjunatha C. S.*
Assistant Professor,
Dept. Of Geography
Karnataka State Open University,
Mysuru, Karnataka

Dhanaraj K.
Assistant Professor - I
Amity Institute Of Geoinformatics And Remote Sensing
Amity University, Noida
Sector 125, Noida, Uttar Pradesh - 201313, India.

Chandrashekara B.
Professor, Department Of Geography
University Of Mysuru
Manasagangothri, Mysuru, Karnataka

Abstract
In the context of rapid urban growth in the small and medium-sized cities of developing countries, the current work attempts to calibrate the CA-based SLEUTH urban growth model to and predict urban growth for the first time in a medium-sized city of Mysuru in southern India. The city has experienced a rapid urban growth in recent times. The current study uses the mixed methodology approach by incorporating the application of remote sensing, GIS, and urban growth model to map, quantify, analyse, and predict urban growth dynamics of Mysuru during the period from 1995 to 2041. The analysis of classified historical urban growth during 2000 to 2020 shows that there is a consistent increase of urban area in Mysuru. The SLEUTH model, calibrated using the historical urban area of 2000-2016, to predict urban growth for the year 2040. The urban growth simulation from SLEUTH shows slope resistance, spread, and road gravity are the foremost factors influencing urban growth in Mysuru. The urban area is expected to increase from 20312.57 Ha in 1995 to 32499.59 Ha by 2041. The growth is expected to reduce in the eastern part due to the resistance effect of slope. The validation of the model output establishes it as acceptable but found limitation to simulate the small patchy and scattered urban growth in the outskirt of the city. The use of the SLEUTH urban growth modeling can be useful for the better understanding of the urban growth process and would therefore aid urban planners to manage the future urban growth sustainably.

Keywords: *Urban growth model, Cellular Automation, SLEUTH Model,*

Date of Submission: 07-01-2024 Date of Acceptance: 17-01-2024

I. Introduction

According to the World Bank, India's urban population is projected to witness a staggering increase of 404 million urban dwellers by the year 2050, making it one of the fastest-urbanizing countries in the world (United Nations, 2018). What makes this growth even more significant is that it is expected to occur primarily in cities with populations of less than one million. This presents a critical opportunity for focused action and intervention in numerous small cities like Mysuru. Unfortunately, policy negotiations in India have largely neglected small cities, as they have been overlooked and excluded from the discussion (Guin, 2019). However, it is essential to acknowledge that the true advantages of urbanization can only be fully realized if small and mid-sized cities are developed with a strong emphasis on sustainability (Hegazy & Kaloop, 2015). This notion is reinforced by the understanding that a significant portion, ranging from 70 to 80 per cent, of India's urban structure slated for completion by 2030 remains to be constructed (Sastry, 2006; Sanke, et al., 2010). In India, this scenario offers a unique chance to intentionally develop sustainable infrastructure and strategically formulate land-use policies that will define the cities of tomorrow. Therefore, small and mid-sized cities like Mysuru hold the key to India's future sustainable development.

Mysuru, a city located in the southern part of India, has experienced significant urban growth and transformation in the past years. This growth has directed in drastic fluctuations in land use and land cover patterns, resulting in various socio-economic and environmental consequences. Comprehending and evaluating these dynamics is essential for proficient urban planning and the promotion of sustainable development in the area. There is a serious dearth of studies on emerging small and mid-sized cities, particularly among the southern Indian cities. The region is diverse within itself, displaying both urban primacy and dispersed, inclusive urbanisation at the same time (Vaddiraju, 2022). The current study, therefore, attempts to fill the gap by examining the subtleties of urban expansion in the mid-sized city of Mysuru. The present study aims to assess the dynamics of land use and land cover changes in the fast-urbanizing areas surrounding Mysuru, using earth observation and Geographic Information System (GIS) techniques. Moreover, the study aims to predict urban growth in the city of Mysuru for theyear 2041 using SLEUTH urban growth model. The results of this study will offer valuable perspectives on the scope and character of urbanization, as well as the related modifications in land use and land cover, encompassing Mysuru.

The exploration of urban expansion and the promotion of sustainable urban development require the creation of models. Advancements in computational power have empowered the formulation of various methods and techniques for modeling the dynamic nature of urban growth and simulating prospective urban scenarios (Batty & Xie, 1994; Feng, Liu, & Batty, 2015. Cellular Automaton (CA) models are considered efficient for simulating urban growth, thanks to their simplicity, structured nature, capacity for evolution, and ability to simulate intricate urban forms and geographical phenomena (Batty, Xie, & Sun, 1999; Xing, Qian, Guan, Yang, & Wu, 2020). The transition rule dictates the cell's state based on the states of its neighbouring cells. SLEUTH, as described by (Clarke, Hoppen, & Gaydos, 1996), is a Cellular Automaton (CA)-based model designed for urban growth modeling. The acronym SLEUTH stands for Slope, Land use, Exclusion, Urban, Transportation network, and Hill shade. This model is composed of two sub-models: the Urban Growth Model (UGM) and the Land-cover Deltatron Model (LCD). Both sub-models operate on a set of predefined growth rules. SLEUTH not only models' future urban growth but also learns from past urban growth or a seed layer. Considering the simplicity and robustness of the SLEUTH model, this study employs the Cellular Automaton-based SLEUTH model to simulate urban growth in the Mysuru.

Study area

Mysuru is a historical city and erstwhile capital and is situated in the southern part of Karnataka state. The district of Mysuru shares its borders with Tamil Nadu to the southeast, Kodagu district to the west, To the north, Mandya district is situated, while the northwest is bordered by Hassan district, and the northeast is adjacent to Bangalore district. The city's geographical coordinates span from 12° 14' 41" to 12° 22' 25" N latitudes and 76° 34' 20" to 76° 43' 23" E longitudes (Fig. 1). The Cauvery River drains the northern region of the city, while the Kabini river drains the southern region. In addition, there are numerous tanks and lakes situated throughout Mysuru city and its outskirts. Additionally, Mysuru boasts numerous tanks and lakes, both within the city and its peripheries, further enhancing its ecological and hydrological significance. The distinctive spatial and environmental attributes of the Mysuru study area establish it as a perfect context for delving into the repercussions of swift urbanization on alterations in land use and land cover. It is a historically significant city known for its rich cultural heritage and is often referred to as the Cultural Capital of Karnataka. Mysuru is governed by a Municipal Corporation and plays a crucial role as an administrative, educational, and economic centre in the region. The city is located approximately 146 km southwest of the state capital, Bengaluru. Mysuru is renowned for its magnificent palaces, including the iconic Mysuru Palace, which attracts tourists from around the world. In recent years, Mysuru has experienced rapid urban expansion and development, leading to various land use and land cover changes (Aithal, Setturu, S, Durgappa, & Ramachandra, 2012). The expansion of residential areas, commercial establishments, and infrastructure projects has transformed the city's landscape. These changes have consequences for the environment, socio-economical aspects, and general sustainability of the city. Considering the unique characteristics and ongoing urbanization dynamics, Mysuru provides an excellent case study for examining the impacts of urban expansion, land use changes, and the need for sustainable planning.

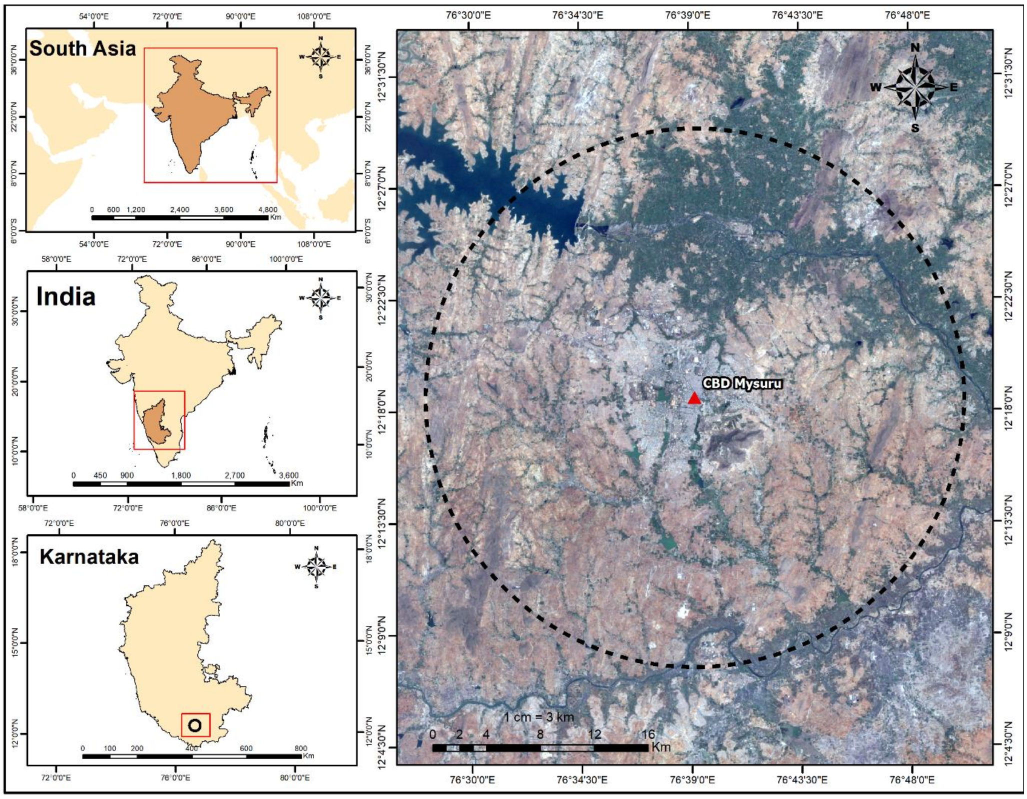

Fig. 1 Location of the study area (Mysuru)

II. Materials and methods

Materials

In this study, a blend of primary and secondary data was employed. The primary data was collected through on-site observations and surveys conducted in the study area. Secondary data, on the other hand, was obtained from various sources. Regarding satellite imagery, a collection of five distinct Landsat images, encompassing TM, ETM+, OLI, and TIRS imageries, was procured from the United States Geological Survey (USGS) (https://earthexplorer.usgs.gov/) to cover the years 1995, 2001, 2007, 2014, and 2022 (Table 1). The selection of these images was grounded in their accessibility, absence of cloud cover, and alignment with seasons that offered optimal visibility of the analysed features. In addition, the secondary data were acquired from various sources, including both physical offices and online platforms. High-resolution images were acquired from Google Earth, while toposheets, city maps, plans, and boundaries were procured from pertinent administrative offices. The demographic data, crucial for the analysis, were collected from the Census of India. Ground observations were undertaken in the study area to collect primary data. This entailed conducting on-site visits to gather GPS reference points, which were subsequently utilized for satellite image classification and precision evaluation. The elevation data, obtained from the USGS Earth Explorer, utilizes the SRTM Digital Elevation Model (DEM). Likewise, the transportation network data for various years in the study area has been acquired from the OpenStreetMap website and extracted through on-screen digitization from topographic sheets.

The forecasting was conducted using the SLEUTH urban growth model within the Cygwin environment. The SLEUTH Model (version 3.0_beta), available at http://www.ncgia.ucsb.edu/projects/gig/index.html, is an open-source modeling package created by Dr. Keith C. Clarke under Project Gigalopolis, USGS, and originally designed for the LINUX operating system. The processing and classification of satellite imagery, along with the examination of changes in land use and land cover and urban expansion, were executed using software including ERDAS Imagine, ArcGIS, and QGIS.

Satellite image pre-processing

These pre-processing techniques are essential to improve the quality and accuracy of the data obtained from satellite images (R, Shenoy, & R, 2017; Asokan, et al., 2020). By applying pre-processing methods, the inherent limitations and distortions in the images can be corrected, allowing for more reliable and meaningful analysis. Landsat collection-2 level-1 datasets are of the highest standard and are considered suitable for time series analysis (EROS, 2020). In this study, atmospheric correction of the Landsat images was conducted by employing the Semi-Automatic Classification Plugin (SCP) within the QGIS 2.6.1 software. The SCP tool facilitated the correction of atmospheric influences present in the satellite images, ensuring more accurate and reliable data for further analysis. To create a comprehensive analysis, the Landsat images were processed by combining their respective bands to generate composite images for each year under investigation (1995, 2001, 2007, 2014, and 2022). Afterward, a segment of the composite image was isolated by extracting the 15 km buffer zone surrounding Mysuru's CBD for each Landsat image, thereby concentrating the analysis on the designated study region.

Satellite image classification

Following the pre-processing stage, the pre-processed satellite data was put under a supervised classification procedure to classify the pixels into distinct LULC classes. Supervised classification involves an expert overseeing the process of pixel assemblage using training sites that provide spectral statistics for each feature type. These training sites are used to guide the computer algorithm in assigning labels to the spectral signatures, categorizing them according to their respective land cover classes (Thenkabail, 2016). The objective of this classification process was to categorize each pixel based on its spectral characteristics and assign it to the appropriate LULC class (Jensen & Cowen, 1999; Thenkabail, 2016). The supervised classification technique employed in this study involved the utilization of known reference samples for training the classification algorithm (Jensen, 2005; Lillesand, Kiefer, & Chipman, 2015).

Table 1 Details of satellite imageries used in the study

Mission	Sensor	Acquisition Date	Spatial Resolution	Path/Row
Landsat 5	TM	22-01-1995	30 m	144/051, 144/052
Landsat 5	TM	12-03-2007	30 m	144/051, 144/052
Landsat 7	ETM +	03-03-2001	30 m	144/052
Landsat 8	OLI TIRS	06-03-2014	30 m	144/052
Landsat 8	OLI TIRS	05-03-2022	30 m	144/052

SLEUTH Model

To operate, SLEUTH necessitates input layers encompassing slope, land-use, urban (seed layer), transportation, and hillshade. The model's urban growth is influenced by four sub-steps or growth rules that dictate distinct growth forms: spontaneous, new spreading center (diffusive), edge (organic), and road-influenced. In turn, these growth rules are determined by five parameters, namely diffusion, breed, spread, slope resistance, and road gravity, each assigned a coefficient value within the range of 0 to 100 (Chaudhuri & Clarke, 2019; Das & Jain , 2022). The model's behaviour is influenced by user-provided excluded layers and slope gradient. Specifically, areas with a slope gradient exceeding 21% are restricted from conversion to urban in accordance with this criterion. The Leesalee metric, generated in the conclusive calibration phase of the model, serves as the basis for selecting the most fitting control parameters. These parameters effectively capture the pattern of urban changes and are subsequently utilized for predicting urban growth (Chaudhuri & Clarke, 2019).

All the necessary input data for the model was organized using ARCMAP 10.3 software. The slope and hillshade layers were derived from SRTM DEM 30 m elevation data in ERDAS IMAGINE. The slope was computed as a percentage, and the hillshade map of the study area was generated. The land-use layer for the model in the study area was created using satellite imagery from the years 2001, 2007 and 2014. The exclusion layer, which designates areas unsuitable for urban growth, was formed by consolidating all water bodies Shapefile derived from the classified land-use land-cover map of the study area. The model necessitates a minimum of one excluded area layer, which, in this case, was developed through the compilation of water bodies. The roads are classified into national and state highways, further categorized as primary, secondary, tertiary roads, and residential roads. All the layers utilized in the model were transformed into Graphics Interchange Format (GIF) raster format with an unsigned 8-bit pixel depth for use in the model. These layers were prepared at spatial resolutions of 30 meters and 100 meters to be employed during the coarse, fine, and final phases of calibration.

SLEUTH Calibration

The model calibration initiates with a test phase, where the model's response to the input datasets is examined by loading the input file directory. Upon successful execution of the test step, the calibration procedure commences. This calibration process involves adjusting the modeled data to align with the historical input datasets. Calibration is conducted in three scenarios: coarse, fine, and final, yielding optimal coefficients (diffusion, breed, spread, slope resistance, and road gravity). These coefficients are then employed by the model to determine the growth rule, enabling effective simulation of urban growth. During the coarse calibration, a scenario file was generated with a broad range of parameter values using the START-STEP-STOP configuration

(0-20-100) (Table 9). The calibration period's start date and end date were established as 2000 and 2016, respectively. During the fine calibration, the parameter range was narrowed, and Monte Carlo iterations were adjusted based on the input raster resolution. The output from the previous calibration served as the basis for further refining the parameter values, and the calibration was conducted with 50 Monte Carlo iterations. The optimal prediction parameters for the urban layer in the end year (2014) obtained from the final calibration were utilized to forecast the urban area in Mysuru for the year 2041.

Prediction and validation

To predict urban growth, the best-fit prediction coefficients were employed to run the prediction mode in SLEUTH for Mysuru. This prediction process utilized 100 m resolution raster input layers with 1000 Monte Carlo iterations. The resulting predicted output GIF images were converted to .tiff format for use in the GIS environment, facilitating further analysis of the forecasted urban growth outcomes.

In the present study, model validation was conducted through the application of statistical measurements and visual inspection techniques. The Kappa index of agreement and correlation coefficient between observed and predicted urban growth pixels were calculated as statistical measures to assess the validity of the model (Foody, 2002). Kappa statistics serve as a metric to quantify the agreement between the observed urban area and the modeled urban area.

$$\text{Kappa} = \frac{P_O - P_C}{1 - P_C}$$

Where, P_o is the proportion of the observed urban pixel and P_c is the expected proportion of correct urban pixels. A Kappa value of 1 signifies that there is a perfect agreement in the data. Subsequently, the correlation coefficient between the historically observed and modeled urban pixels was computed for the years 2001, 2007, 2014, and 2022.

III. Results and discussion

Land use land cover

The land use and land cover maps for the study area in the years 1995, 2001, 2007, 2014 and 2022 were derived through supervised classification of the Landsat images. The classified image (Fig. 3) reveals the presence of five distinct categories of LULC in the study area. These categories include built-up areas represented in red, open land in brown, agricultural land in yellow, vegetation in green and water bodies in blue. The visual analysis of the classified image depicts a consistent pattern of land use and land cover transformation taking place in Mysuru from 1972 to 2018. This observation highlights the dynamic nature of land utilization and underscores the significance of monitoring and understanding LULC changes over time.

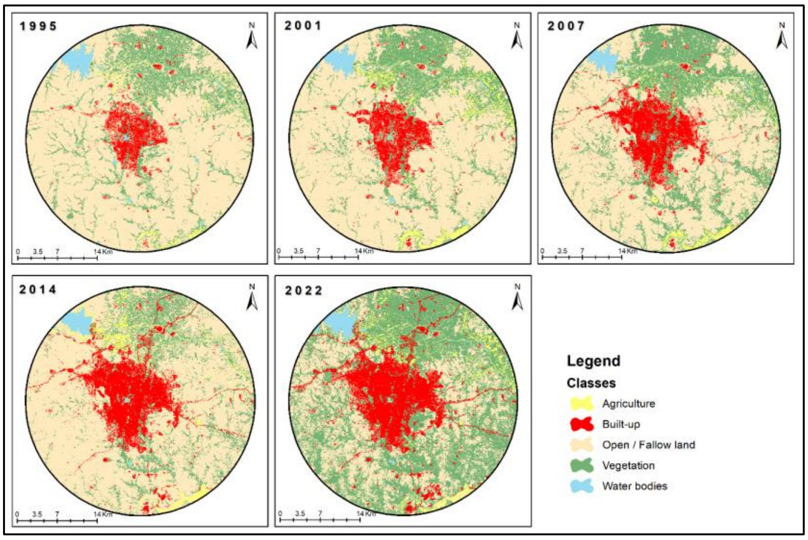

Fig. 2 Land use and land cover of Mysuru in the years 1995, 2001, 2007, 2014 and 2022

Table 2 Dynamic degree of change statistics of different LULC classes in Mysuru for different periods

Classes	Dynamic Degree (%)				
	1995-01	**2001-07**	**2007-14**	**2014-22**	**1995-2022**
Agriculture	13.30	-6.95	8.65	0.27	2.66
Built-up	5.94	9.56	4.05	2.78	8.70

Open/Fallow	-1.25	-1.87	1.57	-6.04	-1.96
Vegetation	2.01	4.81	-5.99	23.42	5.22
Water bodies	-3.73	-1.97	-0.74	2.48	-0.82

SLEUTH calibration and validation

The results of the top three optimal values of growth coefficients during different calibration phases are presented in Table 10. It can be noticed from the table that compare metric, which compares the modelled and real urban extent was high at 0.52. During the coarse calibration, various sets of parameter values were tested. The parameters include population (Pop), edges, clusters, size, Leesalee, Slope%, and others. The values for parameters such as diffusion (Diff), breed (Brd), spread (Sprd), and road gravity (RG) remained consistent across different scenarios, with slight variations in other parameters. In the fine calibration phase, a narrower range of parameter values was explored. The compare value remained constant at 0.64. The metrics assessing the resemblance in shape and form between modeled and actual urban growth—Edge r2 and R2 Cluster—exhibited high values, reaching 0.77 and 0.95, respectively. Additionally, the average x and y values for both modeled and actual urban cells were notably elevated, registering at 0.95 and 0.60, respectively.

Table 3 Broad range of parameter value using start-step-stop configuration in coarse, fine and final calibration

Growth Parametres	Coarse			Fine			Final			Prediction
	Monte Carlo Iterations = 100			Monte Carlo Iterations = 25			Monte Carlo Iterations = 50			
	Total simulation runs = 7770			Total simulation runs = 1600			Total simulation runs = 1023			
	Start	Step	Stop	Start	Step	Stop	Start	Step	Stop	Best Fit
Diffusion	0	20	100	1	5	20	1	3	10	10
Spread	0	20	100	10	5	30	20	3	30	38
Bread	0	20	100	1	5	20	1	3	10	15
Slope Res.	0	20	100	50	5	70	60	3	70	40
Road Gr.	0	20	100	1	10	40	1	8	30	35

The calibration evaluation indices indicate that the chosen coefficients for growth modeling effectively capture the characteristics of actual urban growth in Mysuru. Consequently, these coefficients can be reliably utilized in the prediction phase. Following a successful test run of the SLEUTH model, coarse calibration was conducted, utilizing a range of controlling coefficients from 0 to 20 to 100. Subsequently, during the fine and final calibration steps, the optimal coefficient range was determined by averaging the values, considering the Leesalee metric, as illustrated in Table 9. Following the final calibration, the most optimal coefficients were chosen for the five parameters, and these selected coefficients will be employed in the prediction phase.

Table 4 The top three optimal values for growth coefficients obtained during the coarse, fine, and final phases of the SLEUTH model calibration.

Compare	Pop	Edges	Clusters	Size	Leesalee	Slope%	Urban	Xmean	Ymean	Rad	Fmatch	Diff	Brd	Sprd	Slp	RG
Coarse calibration																
0.52	0.93	0.83	0.94	0.99	0.48	0.63	0.88	0.48	0.34	0.94	0.90	1	1	20	60	1
0.52	0.93	0.83	0.94	0.99	0.48	0.63	0.88	0.48	0.34	0.94	0.90	1	1	20	60	20
0.52	0.93	0.83	0.94	0.99	0.48	0.63	0.88	0.48	0.34	0.94	0.90	1	1	20	60	40
Fine calibration																
0.64	0.93	0.78	0.93	0.99	0.48	0.60	0.88	0.27	0.38	0.94	0.90	1	1	25	65	1
0.64	0.93	0.78	0.93	0.99	0.48	0.60	0.88	0.27	0.38	0.94	0.90	1	1	25	65	11
0.64	0.93	0.78	0.93	0.99	0.48	0.60	0.88	0.27	0.38	0.94	0.90	1	1	25	65	21
Final calibration																
0.60	0.93	0.75	0.95	0.96	0.51	0.05	0.91	0.95	0.60	0.93	0.92	1	1	29	63	25
0.60	0.93	0.75	0.92	0.97	0.51	0.04	0.91	0.96	0.62	0.93	0.92	1	4	29	66	17
0.61	0.93	0.75	0.98	0.96	0.51	0.23	0.91	0.95	0.60	0.93	0.92	1	1	29	60	17

The observed trend in growth coefficients suggests that urban expansion in Mysuru will be significantly influenced by the undulating topography of the region, with a more pronounced deterrent effect of slope, particularly towards the east and northeast where steeper slopes are prevalent due to the undulating terrain. The city is expected to undergo edge growth or urban expansion from existing patches, given the substantial contribution of the spread coefficient. The coefficient value for road gravity indicates that new urban growth is likely to occur in proximity to transportation networks. However, the relatively lower significance assigned to the diffusion and breed coefficients in the study area indicates that the simulation of random spontaneous urban growth and the emergence of new urban centres has a lower likelihood. Nevertheless, the probability of new urban centres emerging and spontaneous urban growth remains relevant, especially along transportation networks. It can be inferred that future urban growth in Mysuru is influenced by the development of the transportation network and investments in creating and expanding new infrastructure services, which would serve as focal points for growth in the study area. The figure 7 shows that the most important driving forces of urban growth in Mysuru are coefficients of slope resistance (40), spread (38) and road gravity (35). The influence of diffusion (10) and bread (15) was relatively lower. The city is expected to undergo edge growth or urban expansion from existing patches, given the substantial contribution of the spread coefficient. Additionally, the coefficient value for road gravity indicates that new urban growth is likely to occur in proximity to transportation networks. The higher values of spread coefficient suggest the rapid spatial expansion of the city towards outskirts.

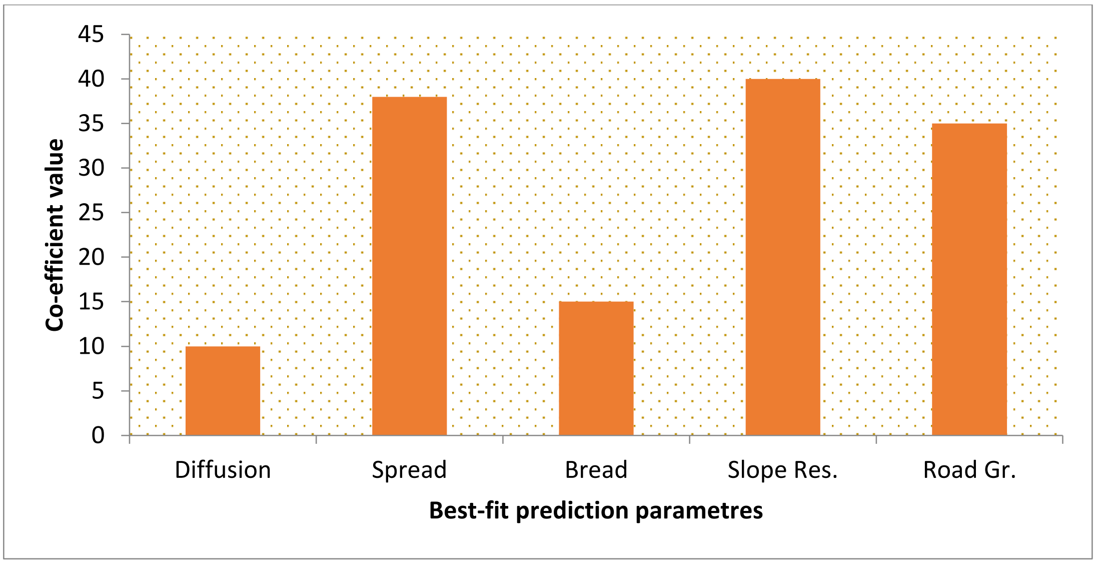

Fig. 3 The best-fit growth parameters for urban growth prediction in Mysuru

Utilizing the optimal parameter coefficients derived from the SLEUTH model calibration based on the historical urban growth data of Mangaluru, a growth prediction for the year 2041 was conducted. According to the SLEUTH model prediction, the city of Mysuru is anticipated to expand from 20,312.57 hectares in 2022 to 32,499.59 hectares by 2041 (Fig. 8). This represents an increase of over 60% in built-up area. The prediction output map illustrating the urban growth of Mysuru from the model is depicted in Fig. 8. The simulation results indicate an anticipated expansion of the city's urban footprint. Notably, substantial growth in the urban area of Mysuru is projected to occur in the surrounding area of the city by the year 2041, consuming agricultural and open land. The urban area has particularly expanded towards the southern part of the city. The expansion could likely be influenced by industrial development and transportation facilities. An evident growth pattern is observable along the transportation network in the study area, notably in the east and along the north-south direction where national highways traverse. This growth aligns with the existing road infrastructure. Additionally, small patches indicating the emergence of spontaneous new urban centers are discernible, particularly influenced by their proximity to roads. Notable instances of such emergence, referred to as "bread points," are noticeable in the southwestern and northeastern corners of the study area. These areas exhibit signs of spontaneous urban development influenced by their connectivity to road networks.

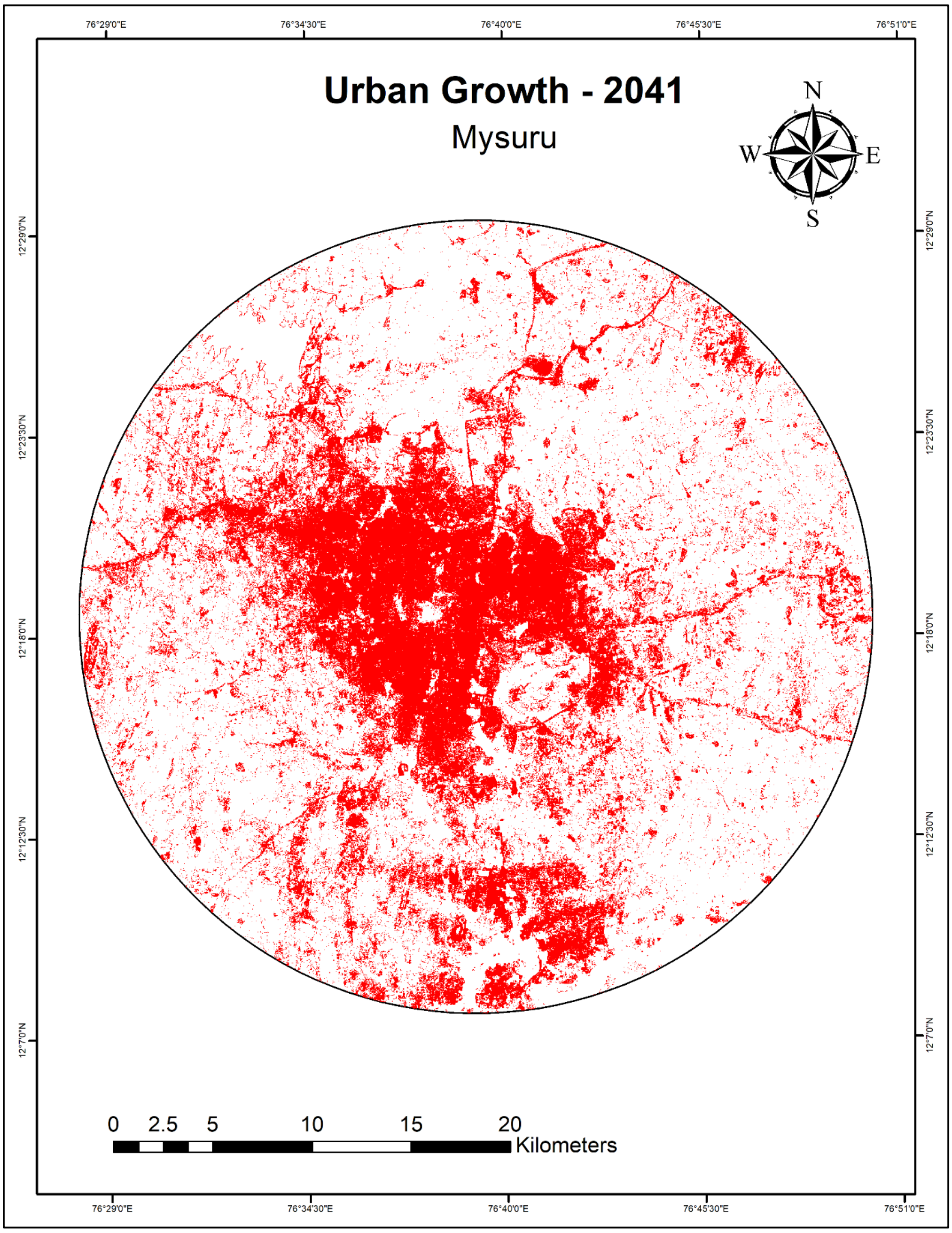

Fig. 4 Predicted urban growth of Mysuru for the year 2041.

The hallmark feature of urban growth in the study area is the expansion of urban areas and the emergence of new urban centers along the highways. Notably, the existing urban centers situated away from the Central Business District (CBD) of the city have undergone substantial and widespread urban growth. This growth unfolds independently starting from 2022 and progressively integrates with the larger urban patch of Mysuru city by the year 2041. For instance, in the southern part of the city, these urban centers merge at a tri-junction, forming an agglomeration that becomes a distinct entity. Similarly, the industrial hotspot area undergoes spatial expansion, incorporating more of the surrounding areas. This spatial transformation reflects the dynamic and evolving nature of urban development in the study area, with key growth nodes emerging along transportation routes and existing urban centers experiencing substantial expansion and integration over time.

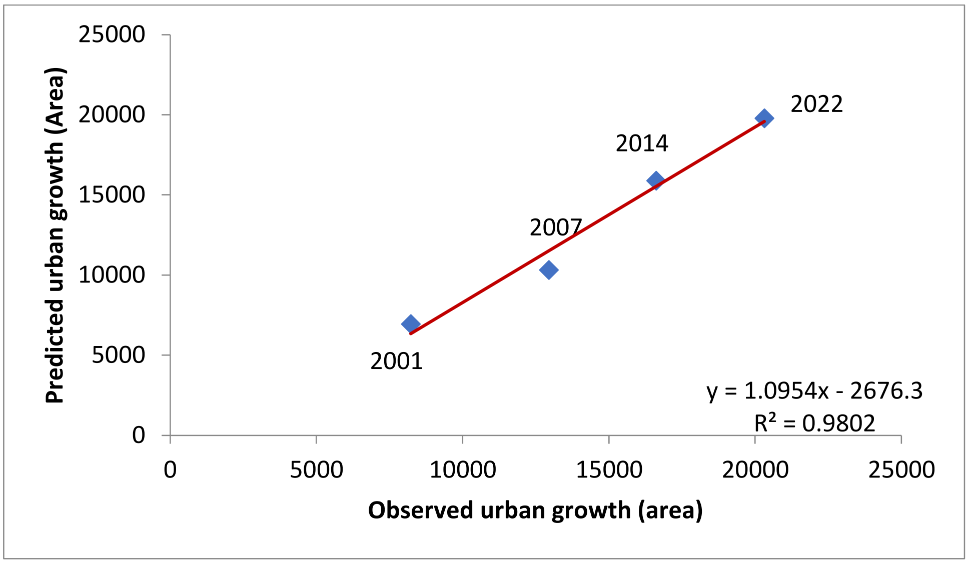

Fig. 5 Shows the observed and predicted urban growth in hectares for Mysuru during 2001-2022

The predicted image is susceptible to errors; therefore, the accuracy of the prediction is typically assessed by comparing it with an observed map. The assessment of the accuracy of the modeled urban growth in Mysuru involves employing statistical measurements, namely the Kappa agreement and correlation coefficient, comparing historical and predicted urban areas. Additionally, a visual comparison of the spatial extents of actual and modeled urban areas is conducted.

The overall accuracy of the modeled urban growth is determined to be 86.44%, indicating a reasonably high level of accuracy in the model's predictions. The Kappa agreement, a statistical measure of agreement, is calculated to be 0.71, which is considered an acceptable value. This suggests that there is agreement between the modeled urban growth and the reference historical urban area.

However, a lower Kappa value for the model output implies a reduced spatial match between the predicted urban area and the observed urban growth. This discrepancy could be attributed to two main factors. Firstly, the coarse spatial resolution of the modeled urban data may contribute to differences when compared to the actual data. Secondly, the absence of certain urban patches in the modeled urban layer may also influence the lower Kappa value. Despite this, the overall accuracy of 86.44% indicates that the model provides a reliable representation of urban growth dynamics in Mysuru.

A robust correlation is evident between the modeled and observed number of urban pixels for the years 2016, 2007, 2014, and 2022, as indicated by a high R-squared (R2) value of 0.98. This high correlation signifies the success of the SLEUTH model in accurately simulating the urban growth area of Mysuru. The R^2 value of 0.98 indicates that approximately 98% of the variation in the observed urban pixels can be explained by the SLEUTH model, reinforcing its effectiveness in capturing and replicating the spatial patterns of urban growth in the study area across multiple time points.

IV. Conclusions

In the current study, a comprehensive dataset of land use and land cover was generated meant for Mysuru, India, utilizing a series of Landsat satellite images spanning a period of 27 years, ranging from 1995 to 2022. The study has helped to effectively monitor, enumerate, and designate the fluctuations in land use and land cover over the time, with a particular focus on variations in built-up areas. This allowed us to identify and analyse the inclinations and patterns of urban expansion. The present work employed a mixture of remote sensing and GIS techniques to accurately capture and analyse the quantitative aspects of LULC modification and the intricate details of built-up expansion. This research is dedicated to the comprehensive analysis and modeling of urban growth patterns and dynamics in Mysuru City, India, spanning the years 1990 to 2040. Given the backdrop of swift urban expansion in small and medium-sized cities within developing nations, this research endeavours to pioneer the calibration and prediction of urban growth using the Cellular Automaton-based SLEUTH model in the medium-sized city of Mysuru in southern India. Mysuru has witnessed a rapid surge in urban development in recent years.

Employing a mixed methodology approach, the study integrates remote sensing, GIS, and the urban growth model to systematically map, quantify, analyse, and predict the dynamics of urban growth in Mysuru over the specified period. Examination of classified historical urban growth from 2000 to 2020 reveals a consistent increase in the urban area of Mysuru. The calibrated SLEUTH model, utilizing data from 2000 to

2016, is deployed to predict urban growth up to the year 2040. The simulation from SLEUTH underscores the prominence of slope resistance, spread, and road gravity as pivotal factors influencing urban growth in Mysuru. Projections indicate an anticipated rise in urban area from 20,312.57 hectares in 1995 to 32,499.59 hectares by 2040. Notably, growth is expected to diminish in the eastern part due to the inhibiting effect of slope resistance. While model validation deems the output acceptable, limitations are acknowledged in simulating small, patchy, and scattered urban growth in the city's outskirts. The application of the SLEUTH urban growth modeling proves invaluable for comprehending the urban growth process, providing urban planners with crucial insights to manage future urban expansion sustainably.

References

[1]. Aithal, B. H., Setturu, B., S, S., Durgappa, D., & Ramachandra, T. V. (2012). Spatial Patterns Of Urbanization In Mysore: Emerging Tier Ii City In Karnataka. Proceedings Of Nrsc User Interaction Meet- 2012. Hyderabad.

[2]. Alberti, M., Weeks, R., & Coe, S. (2004). Urban Land-Cover Change Analysis In Central Puget Sound. Photogrammetric Engineering & Remote Sensing, 1043–1052. Retrieved From Https://Pdfs.Semanticscholar.Org/D2b6/43acab0679224b1071616f2be56305e2449c.Pdf.

[3]. Anderson, J. R., Hardy, E. E., Roach, J. T., & Witmer, R. E. (1976). A Land Use And Land Cover Classification System For Use With Remote Sensor Data. Usgs Professional Paper 964, 138– 145. Retrieved From Http://Pbcgis.Com/Raster/Anderson.Pdf.

[4]. Asokan, A., Anitha, J., Ciobanu, M., Gabor, A., Naaji, A., & Hemanth, D. J. (2020). Image Processing Techniques For Analysis Of Satellite Images For Historical Maps Classification—An Overview. Applied Sciences, 10(12). Retrieved From Https://Doi.Org/10.3390/App10124207.

[5]. Bhatta, B. (2010). Analysis Of Urban Growth And Sprawl From Remote Sensing Data. Heidelberg: Springer.

[6]. Bhatta, B., Saraswati, S., & Bandyopadhyay, D. (2010). Quantifying The Degree-Of-Freedom, Degree-Of-Sprawl,And Degree-Of-Goodness Of Urban Growth From Remote Sensing Data. Applied Geography, 30(1), 96–111. Retrieved From Https://Doi.Org/10.1016/J.Apgeog.2009.08.001.

[7]. Chughtai, A. H., Abbasi, H., & Karas, I. R. (2021). A Review On Change Detection Method And Accuracy Assessment For Land Use Land Cover. Remote Sensing Applications: Society And Environment, 22. Retrieved From Https://Doi.Org/10.1016/J.Rsase.2021.100482.

[8]. Congalton, R. G., & Green, K. (2008). Assessing The Accuracy Of Remotely Sensed Data: Principles And Practices (2 Ed.). Boca Raton: Crc Press. Retrieved From Https://Doi.Org/10.1201/9781420055139.

[9]. Das, S., & Angadi, D. P. (2020). Land Use-Land Cover (Lulc) Transformation And Its Relation With Land Surface Temperature Changes: A Case Study Of Barrackpore Subdivision, West Bengal, India. Remote Sensing Applications: Society And Environment, 19. Retrieved From Https://Doi.Org/10.1016/J.Rsase.2020.100322.

[10]. Eros. (2020, March 4). Usgs Eros Archive - Landsat Archives - Landsat 8-9 Operational Land Imager And Thermal Infrared Sensor Collection 2 Level-1 Data. Doi:10.5066/P9ogbgm6

[11]. Fertner, C., Jørgensen, G., Nielsen, T. A., & Nilsson, K. S. (2016). Urban Sprawl And Growth Management – Drivers, Impacts And Responses In Selected European And Us Cities. Future Cities And Environment, 2. Retrieved From Https://Doi.Org/10.1186/S40984-016-0022-2.

[12]. Foody, G. M. (2002). Status Of Land Cover Classification Accuracy Assessment. Remote Sensing Of Environment, 185–201. Retrieved From Https://Doi.Org/10.1016/S0034-4257(01)00295-4.

[13]. Freeman, L. (2001). The Effects Of Sprawl On Neighborhood Social Ties: An Explanatory Analysis. Journal Of The American Planning Association, 69-77. Retrieved From Https://Doi.Org/10.1080/01944360108976356.

[14]. Garouani, A. E., Mulla, D. J., Garouani, S. E., & Knight, J. (2017). Analysis Of Urban Growth And Sprawl From Remote Sensing Data: Case Of Fez, Morocco. International Journal Of Sustainable Built Environment, 160-169.

[15]. Guin, D. (2019). Contemporary Perspectives Of Small Towns In India: A Review. Habitat International, 86, 19-27. Retrieved From Https://Doi.Org/10.1016/J.Habitatint.2019.02.003.

[16]. Han, L., Zhou, W., Li, W., & Li, L. (2014). Impact Of Urbanization Level On Urban Air Quality: A Case Of Fine Particles (Pm2.5) In Chinese Cities. Environmental Pollution, 194, 163-170. Retrieved From Https://Doi.Org/10.1016/J.Envpol.2014.07.022.

[17]. Harris, P. M., & Ventur, S. J. (1995). The Integration Of Geographic Data With Remotely Sensed Imagery To Improve Classification In An Urban Area. Photogrammetric Engineering & Remote Sensing, 61(8), 993–998. Retrieved From Https://Www.Asprs.Org/Wp-Content/Uploads/Pers/1995journal/Aug/1995_Aug_993-998.Pdf.

[18]. Hassan, Z., Shabbir, R., Ahmad, S. S., Malik, A. H., Aziz, N., Butt, A., & Erum, S. (2016). Dynamics Of Land Use And Land Cover Change (Lulcc) Using Geospatial Techniques:A Case Study Of Islamabad Pakistan. Springerplus, 812. Retrieved From Https://Doi.Org/10.1186/S40064-016-2414-Z.

[19]. Hegazy, I. R., & Kaloop, M. R. (2015). Monitoring Urban Growth And Land Use Change Detection With Gis And Remote Sensing Techniques In Daqahlia Governorate Egypt. International Journal Of Sustainable Built Environment, 117–124. Retrieved From Http://Dx.Doi.Org/10.1016/J.Ijsbe.2015.02.005.

[20]. Ismail, M. H., & Jusoff, K. (2008). Satellite Data Classification Accuracy Assessment Based From Reference Dataset. International Journal Of Geological And Environmental Engineering, 2(3), 23-29. Retrieved From Https://Pdfs.Semanticscholar.Org/D5e0/3bd3a3454bb7cd3757b4a406c1f01d113100.Pdf.

[21]. Jensen, J. R. (2005). Introductory Digital Image Processing A Remote Sensing Perspective. London: Pearson Prentice Hall. Retrieved From Https://Dl.Acm.Org/Doi/Book/10.5555/526335.

[22]. Jensen, J. R., & Cowen, D. C. (1999). Remote Sensing Of Urban/Suburban Infrastructure And Socio-Economic Attributes. Photogrammetric Engineering & Remote Sensing, 65(5), 611-622. Retrieved From Https://Www.Asprs.Org/Wp-Content/Uploads/Pers/99journal/May/1999_May_611-622.Pdf.

[23]. Laidley, T. (2016). The Problem Of Urban Sprawl. Contexts, 15(3), 74–77. Retrieved From Https://Doi.Org/10.1177%2f1536504216662257.

[24]. Lillesand, T. M., Kiefer, R. W., & Chipman, J. W. (2015). Remote Sensing And Image Interpretation (7 Ed.). Westford: Johnwiley & Sons, Inc.

[25]. Liu, C., Xu, Y., Sun, P., Huang, A., & Zheng, W. (2017). Land Use Change And Its Driving Forces Toward Mutual Conversion In Zhangjiakou City, A Farming-Pastoral Ecotone In Northern China. Environ Monit Assess 189, 505. Retrieved From Https://Doi.Org/10.1007/S10661-017-6218-6.

[26]. M, U. S., B, S., & Rego, J. (2021). An Overview Of Agriculture In Mysore District: Proposal Of An Agriculture Hub In Mysore City. International Journal Of Recent Technology And Engineering, 10(4). Retrieved From Https://Www.Ijrte.Org/Wp-Content/Uploads/Papers/V10i4/C64810910321.Pdf.
[27]. Manandhar, R., Odeh, I. O., & Ancev, T. (2009). Improving The Accuracy Of Land Use And Land Cover Classification Of Landsat Data Using Post-Classification Enhancement. Remote Sensing, 330-344. Retrieved From Https://Doi.Org/10.3390/Rs1030330.
[28]. Mathey, J., Rößler, S., Lehmann, I., & Bräuer, A. (2011). Urban Green Spaces: Potentials And Constraints For Urban Adaptation To Climate Change. In O.-Z. K., Resilient Cities. Local Sustainability, Vol 1 (Pp. 479-485). Dordrecht: Springer. Retrieved From Https://Doi.Org/10.1007/978-94-007-0785-6_47.
[29]. Mundoli, S., Manjunath, B., & Nagendra, H. (2014). Effects Of Urbanisation On The Use Of Lakes As Commons In The Peri-Urban Interface Ofbengaluru, India. International Journal Of Urban Sustainable Development. Retrieved From Http://Dx.Doi.Org/10.1080/19463138.2014.982124.
[30]. Pradhan, & Charan, K. (2013). Unacknowledged Urbanisation: The Newcensus Towns Of India. Economic & Political Weekly, 48(36), 43-51. Retrieved From Https://Mpra.Ub.Uni-Muenchen.De/41035/.
[31]. R, S. D., Shenoy, P. D., & R, V. K. (2017). Remote Sensing Satellite Image Processing Techniques For Image Classification: A Comprehensive Survey. International Journal Of Computer Applications, 161(11).
[32]. Sanke, S., Vittal, I., Dobbs, R., Mohan, A., Gulati, A., Ablett, J., . . . Shethy, G. (2010, April). India's Urban Awakening: Building Inclusive Cities, Sustaining Economic Growth. Retrieved January 22, 2020, From Mckinsey&Company: Https://Www.Mckinsey.Com/Featured-Insights/Urbanization/Urban-Awakening-In-India.
[33]. Sastry, G. S. (2006). Urbanisation In A Forward Looking State Of India : Patterns, Issues And Policy. Bangalore: Institute For Social And Economic Change. Retrieved From Https://Pdfs.Semanticscholar.Org/7dff/Fa9ae07e88d046df7c55755f48abb03d7bc5.Pdf?_Ga=2.114942087.1405177501.1586501049-984924764.1586501049.
[34]. Sastry, G. S. (2009). A Model For Sustainable Urbanisation: The Case Of Karnataka. Journal Of Social And Economic Development, 11(2). Retrieved From
[35]. Https://Go.Gale.Com/Ps/I.Do?Id=Gale%7ca213956973&Sid=Googlescholar&V=2.1&It=R&Linkaccess=Abs&Issn=09725792&P=Aone&Sw=W&Usergroupname=Anon%7e16a59413&Aty=Open+Web+Entry.
[36]. Singh, B., Venkatramanan, V., & Deshmukh , B. (2022). Monitoring Of Land Use Land Cover Dynamics And Prediction Of Urban Growth Using Land Change Modeler In Delhi And Its Environs, India. Environmental Science And Pollution Research, 29, 71534–71554. Retrieved From Https://Doi.Org/10.1007/S11356-022-20900-Z.
[37]. Thenkabail, P. S. (2016). Remote Sensing Handbook Remotely Sensed Data Characterization,Classification, And Accuracies. Boca Raton: Crc Press, Taylor & Francis Group.
[38]. United Nations. (2018, May 16). United Nations. Retrieved February 19, 2020, From Department Of Economic And Social Affairs: Https://Www.Un.Org/Development/Desa/En/News/Population/2018-Revision-Of-World-Urbanization-Prospects.Html.
[39]. Vaddiraju, A. K. (2022). Challenges Of Urbanization In South India: Diverse Patterns And Different Trajectories. Journal Of Leadership Accountability And Ethics, 19(1). Retrieved From Http://Www.Isec.Ac.In/Article%20in%20jlae-2022.Pdf.
[40]. Wu, R., Wang, J., Zhang, D., & Wang, S. (2021). Identifying Different Types Of Urban Land Use Dynamics Using Point-Of-Interest (Poi) And Random Forest Algorithm: The Case Of Huizhou, China. Cities, 114, 103202. Retrieved From Https://Doi.Org/10.1016/J.Cities.2021.103202.